



Mechanistic Study and Characterization of Cold-Sprayed Ultra-High Molecular Weight Polyethylene-Nano-Ceramic Composite Coating

Kesavan Ravi, Yuji Ichikawa, Kazuhiro Ogawa, Tiana Deplancke, Olivier Lame, and Jean-Yves Cavaille

(Submitted May 23, 2015; in revised form September 30, 2015)

The cold spray deposition of ultra-high molecular weight polyethylene (UHMWPE) powder mixed with nano-alumina, fumed nano-alumina, and fumed nano-silica was attempted on two different substrates namely polypropylene and aluminum. The coatings with UHMWPE mixed with nano-alumina, fumed nano-alumina, and fumed nano-silica were very contrasting in terms of coating thickness. Nano-ceramic particles played an important role as a bridge bond between the UHMWPE particles. Gas temperature and pressure played an important role in the deposition. The differential scanning calorimetry results of the coatings showed that UHMWPE was melt-crystallized after the coating.

Keywords coating, cold spray, nano-ceramic particle, ultra-high molecular weight polyethylene (UHMWPE)

1. Introduction

In today's world, realization of the potential of polymeric materials in electronics industry, biotechnology, aviation industry, etc. has been tremendous. Polymer coatings, in general, are one of the most widely used surface improvisation methods in the modern world. They have a variety of applications like surface protection from corrosion (Ref 1), protection from cavitation erosion or mechanical impacts (Ref 2), electronic applications (Ref 3), packaging (Ref 4), and biocompatible membrane (Ref 5). Polymers are being used for various applications due to the need for materials with low cost and high strength to weight ratio.

Ultra-high molecular weight polyethylene (UHMWPE) is characterized by high molecular weight, which makes it known to have exceptional physical and mechanical properties. It has an excellent wear resistance

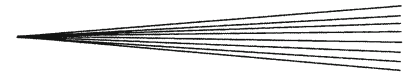
and is commonly used for total joint implants (Ref 6). UHMWPE coatings are envisioned to cater to the problems caused by durability of the slide member in prosthetic joints and subsequently prolong its life (Ref 7). It also has an excellent resistance to impacts and is a material of choice for body armors (Ref 8). It has a large elongation at break (typically several hundred percent) and, as a result, a great ability to absorb energy before fracture (Ref 9).

Due to the high molecular weight of UHMWPE, it exhibits a very high viscosity in the melt region. Thus, the processing by conventional techniques such as injection molding or extrusion becomes impossible. Hence, special fabrication techniques like compression molding or sintering are used, at present, to process UHMWPE (Ref 9). For large-scale productions and for non-planar surfaces, sintering compression is difficult to be used. Hence, a projection technique of solid particles like cold spray was chosen as a better alternative. In this study, cold spray technique is being observed as a potential technique to coat UHMWPE on to different materials.

Cold spraying (CS) involves the impact of powder particles on to a target at very high speeds (500 to 1500 m/s) to form coatings or solid components. It was originally developed in the mid-1980s at the Institute of Applied Mechanics of the Siberian Branch of the Russian Academy of Science (ITAM SB RAS) in Novosibirsk by Papyrin and co-workers (Ref 10) for metallic powders. The accelerating gas may be heated, mainly to achieve higher particle velocities. The powder particles, usually in the particle size range from 5 to 100 μm , are accelerated by injection into a high-velocity stream of gas. The high velocity gas is generated through the expansion of a pressurized preheated gas, which is accelerated to supersonic velocity, with an accompanying decrease in pressure and temperature, through a converging-diverging nozzle

This article is an invited paper selected from presentations at the 2015 International Thermal Spray Conference, held May 11-14, 2015, in Long Beach, California, USA, and has been expanded from the original presentation.

Kesavan Ravi, Yuji Ichikawa, and Kazuhiro Ogawa, Fracture and Reliability Research Institute, Tohoku University, 6-6-11-720, Aoba, Aramaki, Aoba-ku, Sendai 980-8579, Japan; and **Kesavan Ravi, Tiana Deplancke, Olivier Lame, and Jean-Yves Cavaille**, Materials Engineering and Science (MATEIS), CNRS, INSA-Lyon UMR5510, Université de Lyon, 69621 Villeurbanne, France. Contact e-mail: kesavan_ravi@rift.mech.tohoku.ac.jp.



(Ref 11-13). The accelerated particles are then impacted onto the substrate after exiting the nozzle. The major advantage of the cold spray process is that it is a solid-state process, which results in many unique and high-quality coating characteristics.

A very few works have been done with polymer particles as feedstock in thermal spray/cold spray (Ref 14-18) mainly because polymer deposition is difficult to achieve. In this study, the UHMWPE feedstock powder was mixed with different nano-ceramic powders like nano-alumina, fumed nano-alumina, and fumed nano-silica. Nano-ceramic additives were chosen, as it is a well-known filler material in many polymer composites. Addition of fillers to thermoplastic matrix has been found to improve some mechanical properties, such as fracture strength (Ref 19), and friction and wear behavior (Ref 20, 21), as well as thermal stability (Ref 22), flame retardancy (Ref 23), barrier properties (Ref 24), and conductivity (Ref 25). A previous study has also shown improvement in the coating quality when fumed nano-alumina was added to the UHMWPE feedstock (Ref 26).

The major objective of this study is to mechanistically understand the cold-sprayed UHMWPE coatings obtained when different kinds of nano-ceramic particles are added to the feedstock.

The paper is devoted to an investigation of the UHMWPE-nano-ceramic composite coatings by cold spray technique.

2. Experimental

2.1 Cold Spray

The UHMWPE powder was deposited on each of the substrates using downstream injection cold spray technique. Figure 1 shows the schematic of the downstream injection cold spray apparatus used in the experiment. Pressurized gas (air) from 0.2 to 0.8 MPa was supplied from a compressor, which meets the powder particles at the nozzle region. The gas temperature can be varied from room temperature to 500 °C. The powder particles were fed from a vibrating powder feeder at a steady controllable rate. Feed rate was not calculated as the vibratory feeder was used. The air stream containing the polymer particles was then passed through a de Laval nozzle of length 200 mm to deposit onto Aluminum (Al) and Polypropylene (PP) substrates. The nozzle was held right angles to the target with a standoff distance varied from 5 to 20 mm. Table 1 specifies the unit specification of the system.

To control the standoff distance between the nozzle and substrate surface and also to control the traverse parameters, the cold spray unit was mounted on a XYZ stage and manipulated by a personal computer. Figure 2 shows the photograph of the experimental setup.

2.2 Ultra-High Molecular Weight Polyethylene: Structural and Physical Characterization

UHMWPE used in this study is GUR 4170 obtained from Ticona (Oberhausen, Germany). It is in the form of powder with an average size distribution of 60 μm . Figure 3 shows the SEM image of the UHMWPE powder used in this study. The molecular mass deduced from viscosity measurements is 10.5 Mg/mol. The crystallinity ratio was measured by differential scanning calorimetry (DSC) using a Rigaku apparatus at a heating rate of 10 °C/min. The temperature and heat flow scales were calibrated using high-purity alumina.

The nascent powder, rebound particles, and the deposited particles were analyzed by the DSC (Rigaku Thermo plus EVO2) to understand the difference in each of their thermal history. The rebound particles were collected after the cold spray. On the other hand, the deposited particles on Al and PP substrates were scraped off from the coatings to be analyzed. The reference material used in the analysis was Al_2O_3 , which was also used to calibrate the instrument. The polymer samples were heated at a heating rate of 10 °C/min in the range of temperature 70-200 °C, and the subsequent DSC curve was plotted.

The morphological investigations were performed by field emission scanning electron microscope (FE-SEM) using a Hitachi SU-70 operated at 20 kV. A thin Pt coating was applied prior to SEM observation by ion sputtering.

2.3 Nano-ceramics Powders

The nano-ceramic powders used in this study are nano-alumina, fumed nano-alumina, and fumed nano-silica, which are commercially available. Nano-alumina of particle size ~50 nm used is obtained from Sigma Aldrich Japan G. K. Fumed nano-alumina of particle size ~10 nm and fumed nano-silica of particle size ~15 nm were obtained from Degussa.

Figure 4(a-c) shows the TEM images of the nano-alumina (procured from Sigma-Aldrich® website), fumed nano-alumina, and fumed nano-silica, respectively.

2.4 Powder Preparation

In this experiment, 3.8-4% by weight of nano-alumina, fumed nano-alumina, and fumed nano-silica powder were mixed with the UHMWPE powder before the feeding process for each set of experiments. The percentage by weight of nano-particles used in the experiment was considered based on the assumption of 100% surface coverage of UHMWPE particles with a single layer of nano-particles, as suggested in the research article by Yang et al. (Ref 27).

Powders were hand mixed and no special mixing process was used.

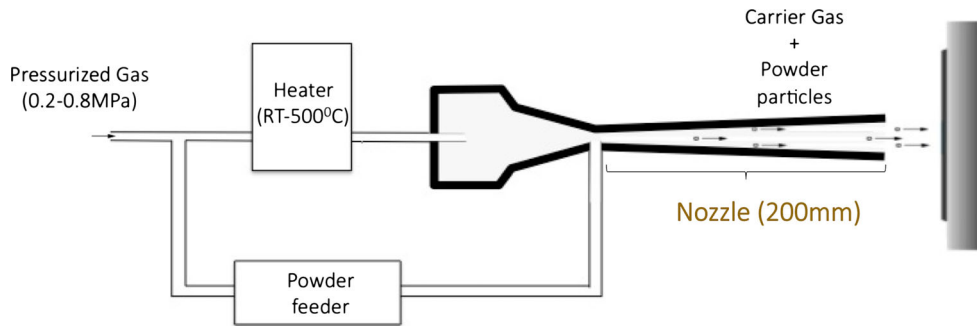


Fig. 1 A schematic of a typical low-pressure downstream injection cold spray system

Table 1 Unit specification of low-pressure downstream injection cold spray system

Parameter	Description
Power	220 V, 3.3 kW
Pressure of consumed air	0.2-1.0 MPa
Consumption of compressed air	0.4 m ³ /min
Temperature range	Room temperature—500 °C (5 modes)
Number of powder feeders	3

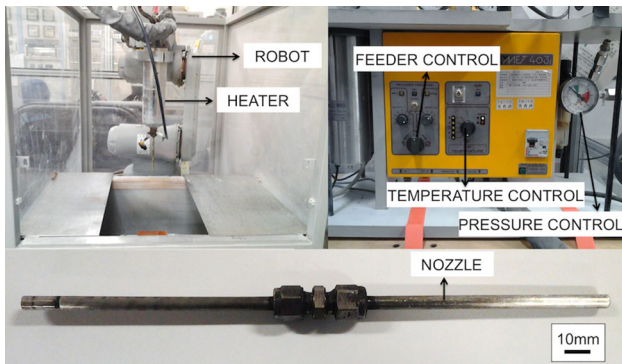


Fig. 2 Photograph of the experimental setup

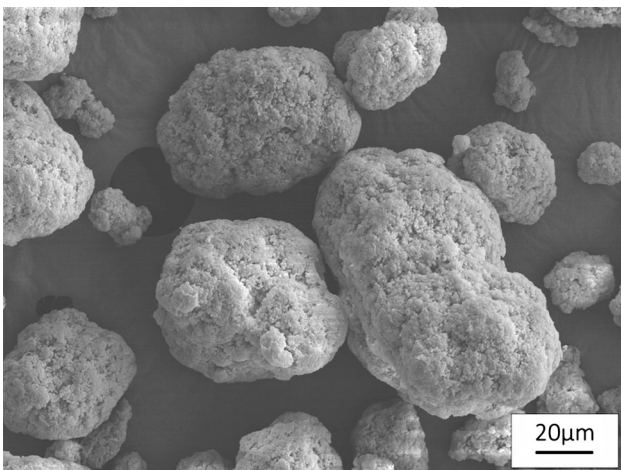


Fig. 3 SEM image of the UHMWPE

3. Results

3.1 Cold Spray with Nano-alumina Addition

The deposition behavior of the UHMWPE-nano-alumina mixture largely depended on the gas temperature and pressure. It was observed that deposition of the polymer-nano-composite mixture occurred when the temperature of the gas was close to 350 °C and gas pressure between 0.3 and 0.4 MPa in the case of Al substrate. On PP substrate, the deposition was observed at 170 °C gas temperature and 0.3-0.4 MPa gas pressure.

At the gas temperature and pressure below the observation of deposition, rebounding of the particles took place. Above this temperature, the system clogged due to molten UHMWPE particles. At high pressures (>0.5 MPa), the rebounding of the UHMWPE particle was accompanied by erosion of substrate.

Figure 5(a) and (b) represents the deposition behavior of the UHMWPE-nano-alumina mixture at different gas temperatures and pressures on Al and PP, respectively.

After a careful tuning of the cold spray parameters, a coating of 70-100 µm thicknesses was obtained on both Al and PP substrates. Figure 6(a) and (b) shows the SEM/EDX images of the coating obtained on Al and PP substrates, respectively.

3.2 Cold Spray with Fumed Nano-alumina Addition

The deposition behavior of the UHMWPE-fumed nano-alumina mixture also largely depended on the gas temperature and pressure. The deposition occurred at similar gas temperature and pressure conditions as that of cold spray with nano-alumina addition.

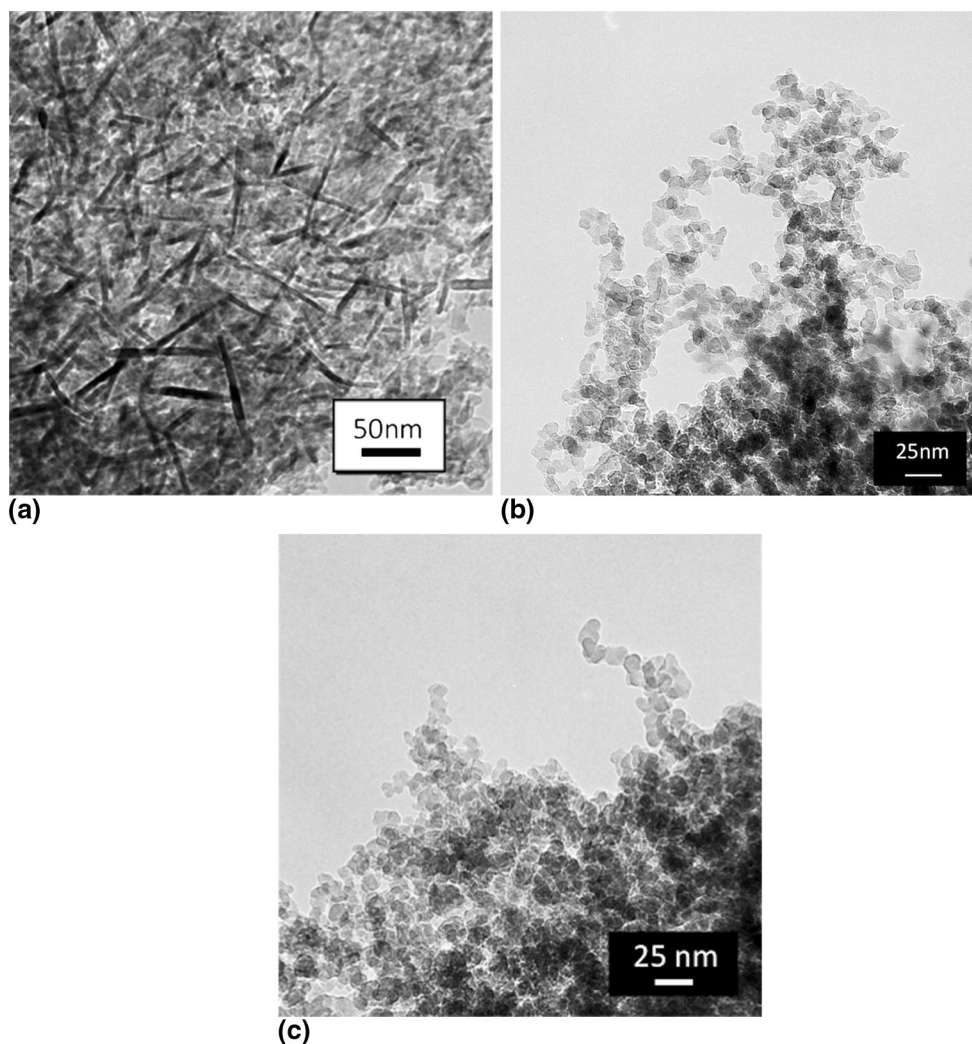


Fig. 4 (a) TEM image of the nano-alumina used in this study (image from Sigma-Aldrich® website). (b) TEM image of the fumed nano-alumina used in this study. (c) TEM image of the fumed nano-silica used in this study

The coating thickness of 3-4 and 1 mm thicknesses were obtained on Al and PP substrates, respectively. Figure 7(a) and (b) shows the photographs of the coating obtained on Al and PP substrates, respectively.

The UHMWPE coating on Al was observed to delaminate when cut. Hence, the coating was heat treated at 200 °C for 10 min in order to improve the adhesion. The samples were then cut and the cross section of the deposit was observed under SEM. Figure 8(a) and (b) shows the cross-sectional SEM/EDX images of the coating on Al and PP substrates, respectively.

3.3 Cold Spray with Fumed Nano-silica Addition

Fumed nano-silica was mixed with UHMWPE and cold sprayed on to Al and PP substrates, respectively. It was observed that deposition of the UHMWPE-fumed nano-silica mixture was not possible on Al substrate at all the

gas temperature and pressure conditions tested. On PP substrate, the deposition was observed at 170 °C gas temperature and 0.3-0.4 MPa gas pressure. Figure 9(a) and (b) represents the deposition behavior of the UHMWPE-fumed nano-silica mixture at different gas temperatures and pressures on Al and PP, respectively.

A coating thickness 70-150 μm thickness was obtained on PP substrate. It was very interesting to observe that there was no coating on Al substrate. The UHMWPE particles tend to rebound when cold sprayed on to Al substrate.

The coating formation in the cold spray involved the interaction of the composite particles with the substrate surface. However, the UHMWPE-fumed nano-silica composite particles interaction with Al surface did not result in a bond formation.

Figure 10 shows the cross-sectional SEM/EDX image of the coating on PP substrate.

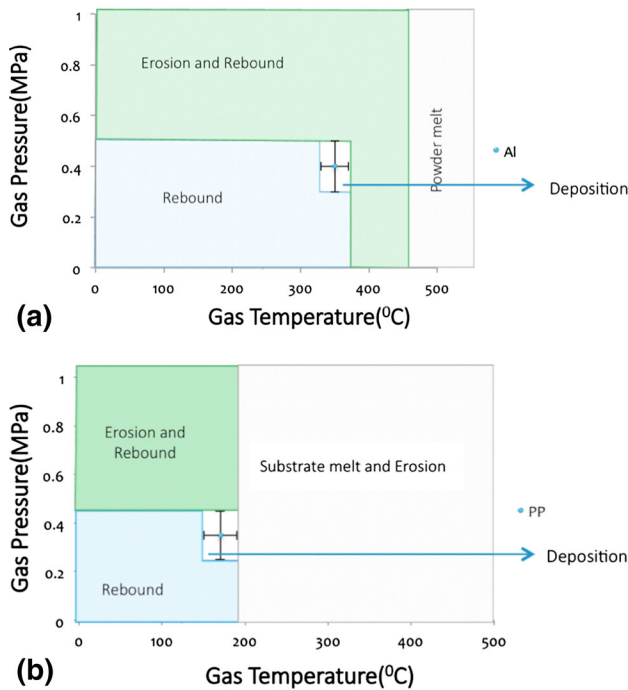


Fig. 5 (a) Deposition behavior of the UHMWPE-nano-alumina mixture at different gas temperatures and pressures on Al. (b) Deposition behavior of the UHMWPE-nano-alumina mixture at different gas temperatures and pressures on PP

4. Discussion

4.1 Effect of the Nano-ceramic Particle

The nano-ceramic particles in the deposits were observed to have settled down at the particle/particle interfaces, which can be seen from the EDX images in Fig. 6, 8, and 10. The basic effect seen after each of the type of nano-ceramic addition is the creation of a bridge bond between the polymeric grains. Figure 11 shows a simple illustration of the possible activation of the polymer grains by the nano-ceramic particles. Due to its high dispersability, nano-ceramic particles settled along the grains of the UHMWPE particles after the mixing forming a composite particle. The composite particles are then cold sprayed on to the desired substrate. The particle/particle interaction takes place during the passage of the composite particles along the nozzle length creating an aggregate of the composite particles. This aggregation is possible by the presence of nano-ceramic particles.

The observance of different coating thicknesses may be attributed to the strength of this bridge bond. Factors affecting the strength of the bond can be narrowed down to the surface properties of each nano-ceramic particles. For example, the hydroxyl groups at the surface of the fumed nano-alumina particle (Ref 28) may play an important role in introducing new bonds like hydrogen bonds between the polymeric grains although it is difficult

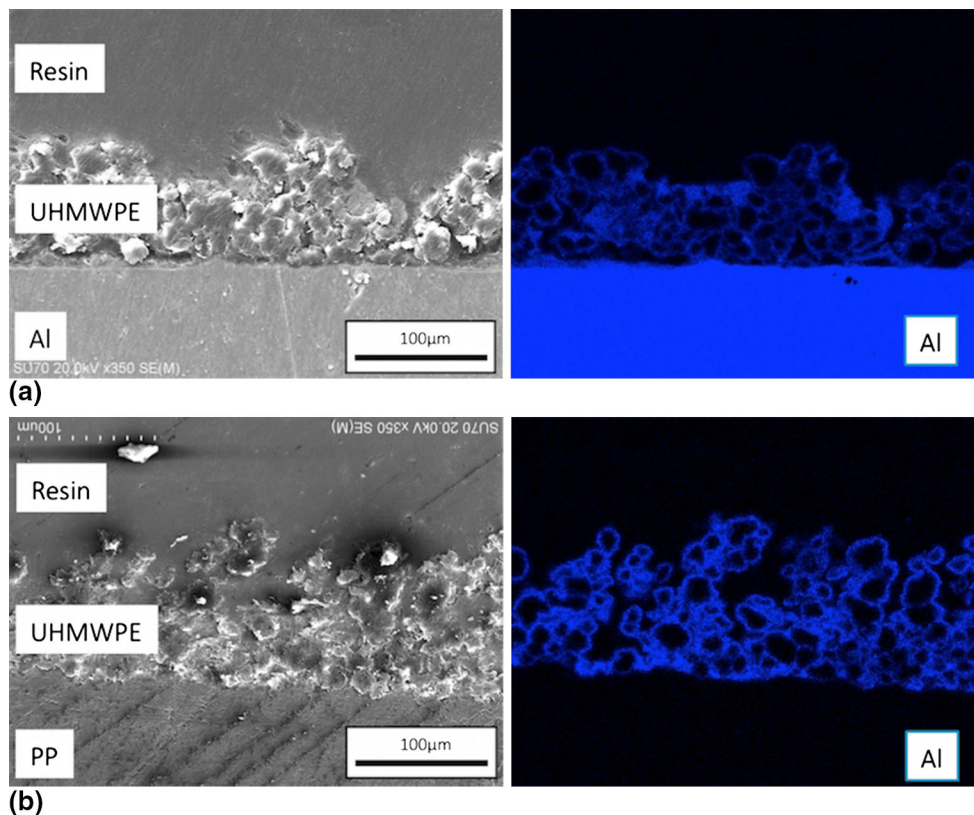


Fig. 6 (a) Cross-sectional SEM/EDX images of the UHMWPE-nano-alumina coating on Al. (b) Cross-sectional SEM/EDX images of the UHMWPE-nano-alumina coating on PP substrate

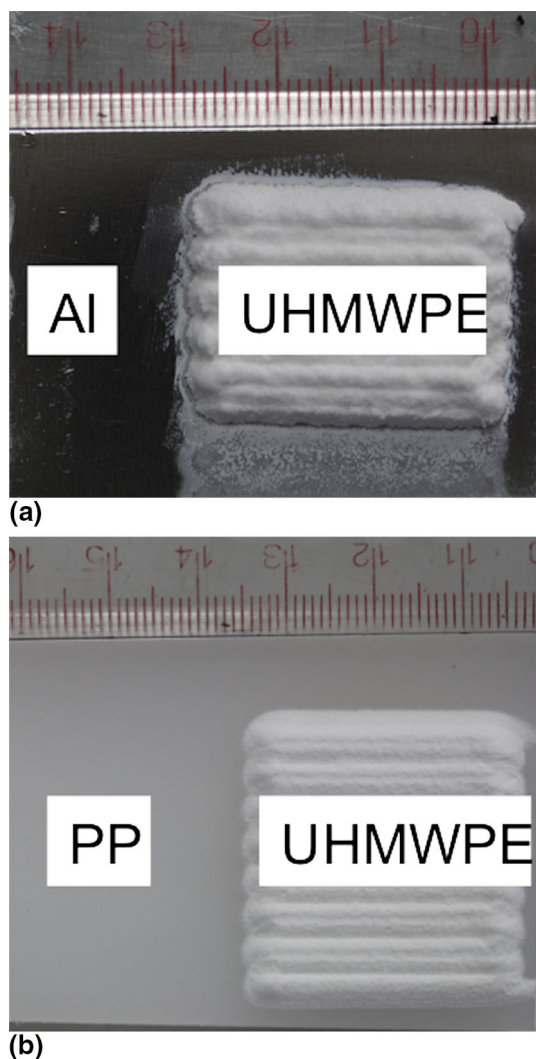


Fig. 7 (a) Photograph of the UHMWPE-fumed nano-alumina coating on Al. (b) Photograph of the UHMWPE-fumed nano-alumina coating on PP

to confirm until future experiments are performed. The presence of such bonds can reinforce the UHMWPE particle-particle bonding. This is significant when the coating quality of UHMWPE-nano-alumina coatings and UHMWPE-fumed nano-alumina coating is compared. Figure 12 shows a simple illustration of the possibility of introduction of extra bonds like hydrogen bonding between the polymer grains. Since the nano-ceramic particles cover the surface of UHMWPE particles, the flowability of UHMWPE-nano-alumina and UHMWPE-fumed nano-alumina mixture will be dependent on the surface charge of nano particles and is considered to be same as both nano-alumina and fumed nano-alumina carry positive charge on their surfaces (Ref 29, 30).

Another parameter that might have interfered in the coating formation would be the surface charge of the nano particles added to the feedstock. For example, the inability of coating formation of UHMWPE-fumed nano-silica powders on Al substrate may be attributed to the negative

surface charge of the fumed silica nano-particles (Ref 31), which may have led to an ineffective particle-substrate electrostatic interaction and/or the chemical dissimilarity between SiO_2 nano-particles and the Al substrate.

Effect of the nano-particles in strengthening of the microstructure is observed as the nano-particles facilitated in the bonding of the UHMWPE particles together. The nano-particles form an interconnected network at the surface of the UHMWPE particles. The presence of nano-ceramic particles must have definitely increased the hardness of the coating. But as the percentage added to the feedstock is very low (~4%), it is not expected to increase drastically. Additionally, the hammering effect is not likely as the mass of the nano-ceramic particles is negligible as compared to that of UHMWPE particles. Hence, the inertia of nano-particles will also be negligible as compared to the polymer particle.

4.2 Deposition Criteria

From Fig. 5 and 9, it is possible to deduce that the deposition window for the UHMWPE does not change when different nano-ceramic particles are used. This leads to a conclusion that the temperature effect on the UHMWPE is very significant. Hence, the thermal history of the particles was analyzed using a DSC.

It is possible to determine whether the nascent UHMWPE particles are crystal melted once after the passage through the nozzle by using DSC. Hence, the thermal state of UHMWPE particles during the impact in the cold spray process can be understood. Figure 13 shows the DSC curves of both the nascent powder and of particles crystallized from the melt UHMWPE. The much higher crystallinity and melting point are characteristic of the special structure UHMWPE nascent reactor powders (Fig. 13). The high melting temperature is attributed to the non-equilibrium chain conformations: the presence of chain-extended crystals as well as constrained chain folded crystals has been proposed (Ref 9, 32, 33).

The melting temperatures and crystallinity of the rebound particles were seen to be similar to that of the nascent powder which can be seen from the DSC curves of the rebound particles at all the gas temperatures. Figure 14 represents the DSC curves for the rebound particles. So the rebounding particles are in the nascent state.

On the other hand, the DSC curves for the deposited particles were observed to have a lower crystallinity and melting temperature than that of the nascent powder (Fig. 15). The deposited particles were observed to be melting during the cold spray experiment, and after recrystallized during the cooling.

During the cold spray, the only region where the particles are heated is the nozzle region where the particles interact with the heated carrier gas. But, this particle-carrier gas interaction time is extremely small. According to the DSC curves of the rebounding particles, the softening of the particles by the carrier gas has not taken place. On the other hand, the DSC curves of the deposited particles show that the heated carrier gas has successfully softened the UHMWPE particles.

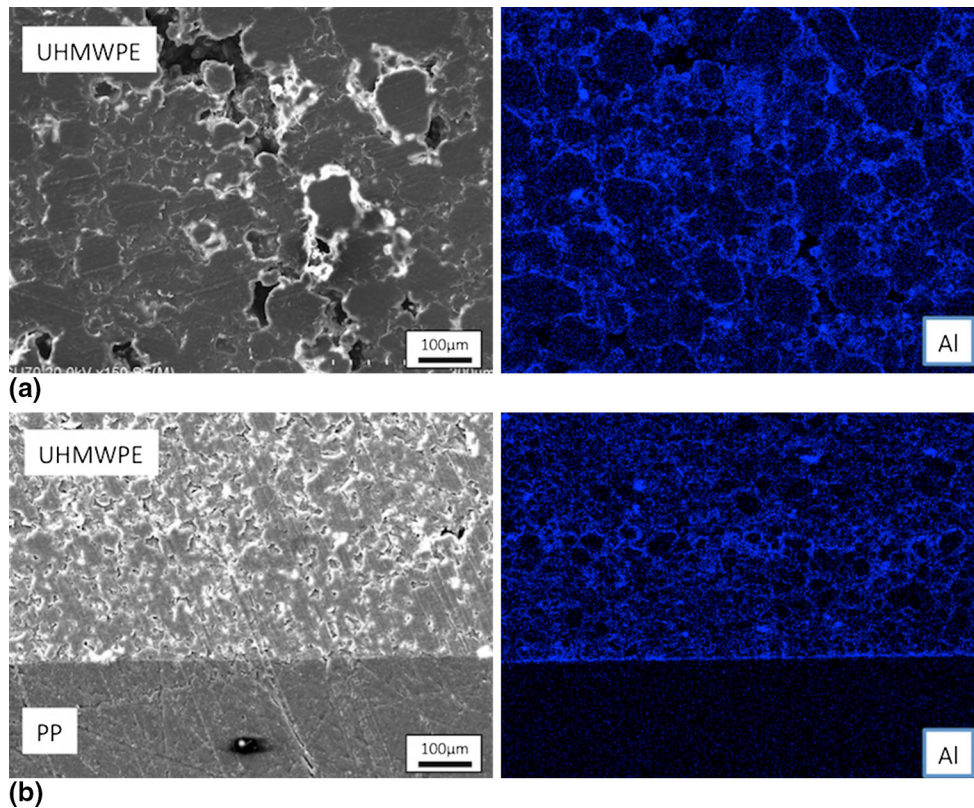


Fig. 8 (a) Cross-sectional SEM/EDX images of the UHMWPE-fumed nano-alumina coating on Al. (b) Cross-sectional SEM/EDX images of the UHMWPE-fumed nano-alumina coating on PP substrate

Hence, in order for the deposition to occur, the UHMWPE particle temperature should be more than 135 °C, rendering it amorphous in structure.

5. Conclusions

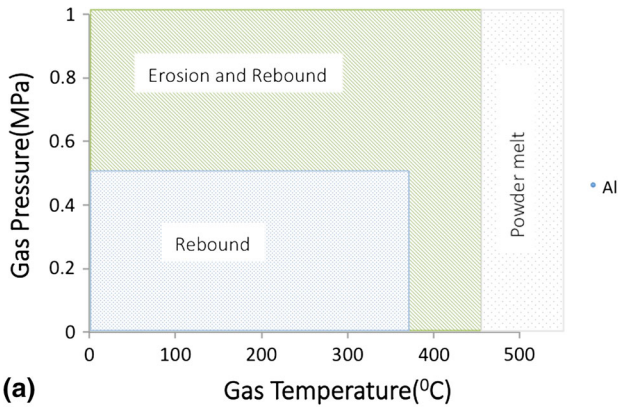
This study analyzes different UHMWPE-nano-ceramic composite coatings. Following conclusions can be drawn from the experiments conducted.

UHMWPE coatings of 4 and 1 mm thickness were achieved on Al and PP substrates, respectively, with the addition of fumed nano-alumina and with the incorporation of 200-mm-long nozzle. Cold spray of UHMWPE-nano-alumina yielded a coating of 70-100 µm on Al and PP substrate and UHMWPE-fumed nano-silica mixtures yielded a coating of 70-150 µm on PP substrate. The addition of nano-ceramic particles to the feedstock UHMWPE aided in effectively building up the coating

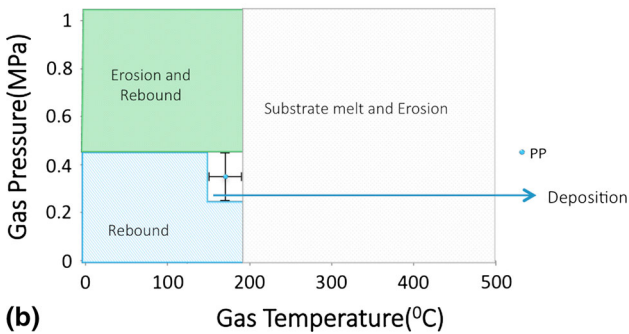
thickness probably due to its role in creating a bridge bond between UHMWPE particles. Nano-particles created a network of finely dispersed particles, which were strongly bonded, to the polymer matrix. The presence of hydroxyl groups and the surface charge at the surface of the nano-ceramic particles may have assisted in a better reinforcement in bonding between the UHMWPE particles.

UHMWPE particles experience crystal melting during its passage through the nozzle region, which is believed to play an important role in its deposition. However, the complete understanding of the deposition mechanism requires further works already ongoing.

This research work is intended to reveal the major differences in the cold-sprayed coating behavior when different kinds of nano-ceramic particles are added as additives to the UHMWPE feedstock. This is the initial step of a larger study. Further studies would help in confirming the exact mechanism behind the coating formation.



(a)



(b)

Fig. 9 (a) Deposition behavior of the UHMWPE-fumed nano-silica mixture at different gas temperatures and pressures on Al and. (b) Deposition behavior of the UHMWPE-fumed nano-silica mixture at different gas temperatures and pressures on PP

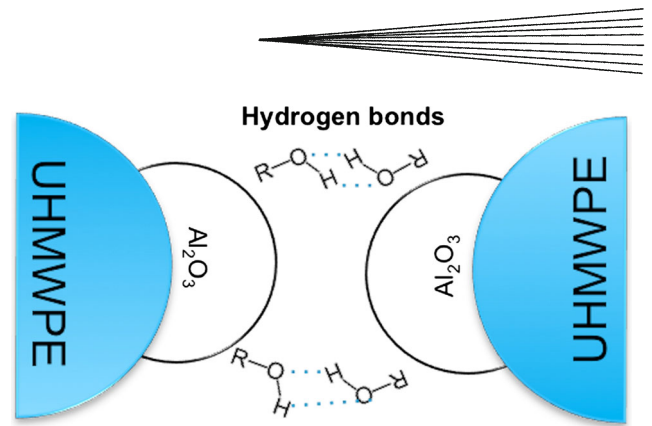


Fig. 12 Illustration of possible extra bonds introduced by hydroxyl group at the fumed nano-alumina surface

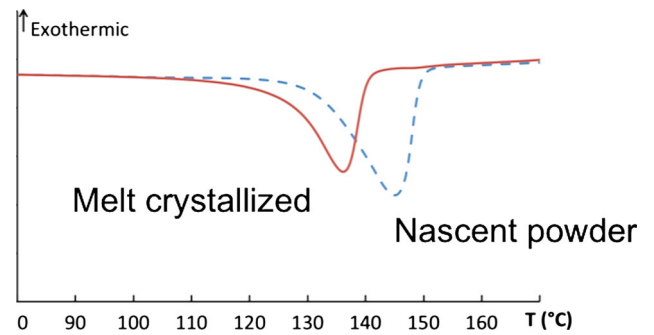


Fig. 13 DSC curves of the nascent powder and the melt-crystallized UHMWPE (Ref 34)

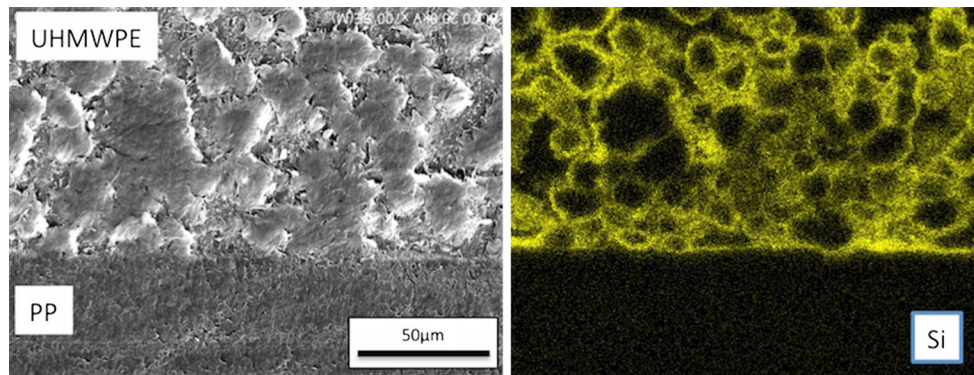


Fig. 10 Cross-sectional SEM/EDX images of the UHMWPE-fumed nano-silica coating on PP substrate

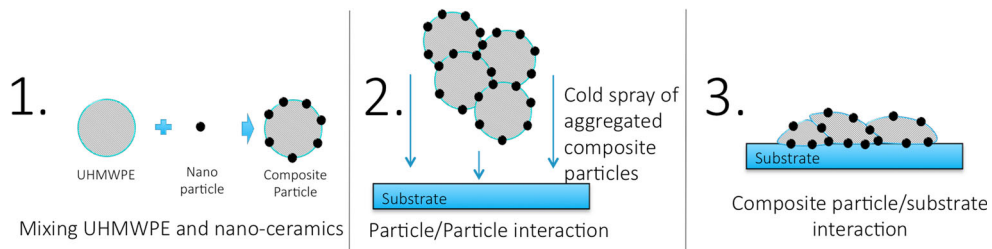


Fig. 11 Illustration of possible activation of the UHMWPE grains by the nano-ceramics mixing

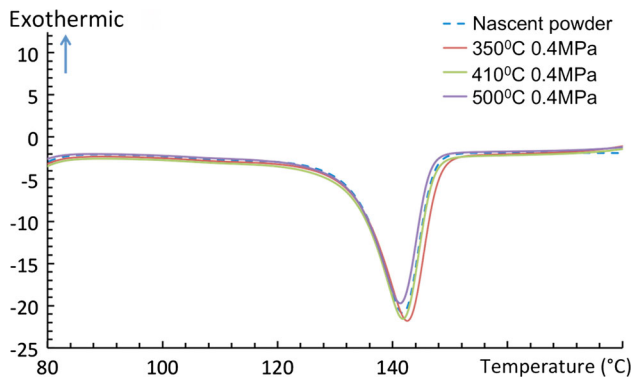


Fig. 14 DSC curves of the rebounded particles at various gas temperatures

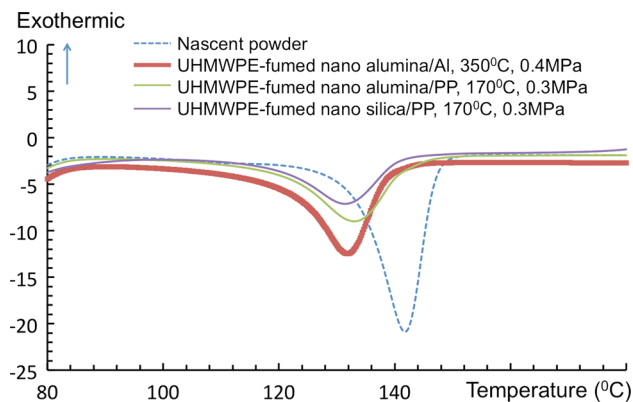


Fig. 15 DSC curves of the deposited particles

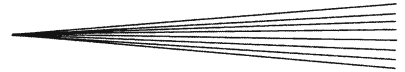
Acknowledgment

The authors are indebted to Ticona (Oberhausen, Germany) for the generous supply of the UHMWPE sample together with its molecular characteristics. This work was partly supported by the JSPS Core-to-Core Program, A. Advanced Research Networks, “International research core on smart layered materials and structures for energy saving.”

References

- S.P. Sitaram, J.O. Stoffer, and T.J. O’Keefe, Application of Conducting Polymers in Corrosion Protection, *J. Coat. Technol.*, 1997, **69**(866), p 65-69
- Y.Q. Wang, L.P. Huang, W.L. Liu, and J. Li, The Blast Erosion Behaviour of Ultrahigh Molecular Weight Polyethylene, *Wear*, 1998, **218**(1), p 128-133
- L.L. Lin, T.H. Ho, and C.S. Wang, Synthesis of Novel Trifunctional Epoxy Resins and their Modification with Polydimethylsiloxane for Electronic Application, *Polymer*, 1997, **38**(8), p 1997-2003
- G. Scott, *Polymers and the Environment*, Vol 19, Royal Society of Chemistry, Cambridge, 1999
- A.G. Mikos, G. Sarakinos, J.P. Vacanti, R.S. Langer, and L.G. Cima, U.S. Patent No. 5,514,378, U.S. Patent and Trademark Office, Washington, DC, 1996

- S.M. Kurtz, *The UHMWPE Handbook: Ultra-High Molecular Weight Polyethylene in Total Joint Replacement*, Academic Press, New York, 2004
- A. Wang, A. Essner, V.K. Polineni, C. Stark, and J.H. Dumbleton, Lubrication and Wear of Ultra-High Molecular Weight Polyethylene in Total Joint Replacements, *Tribol. Int.*, 1998, **31**(1), p 17-33
- D.C. Prevorsek, Y.D. Kwon, and H.B. Chin, Analysis of the Temperature Rise in the Projectile and Extended Chain Polyethylene Fiber Composite Armor During Ballistic Impact and Penetration, *Polym. Eng. Sci.*, 1994, **34**(2), p 141-152
- T. Deplancke, O. Lame, F. Rousset, I. Aguilu, R. Seguela, and G. Vigier, Diffusion Versus CocrySTALLIZATION of Very Long Polymer Chains at Interfaces: Experimental Study of Sintering of UHMWPE Nascent Powder, *Macromolecules*, 2013, **47**(1), p 197-207
- A. Papyrin, Cold Spray Technology, *Adv. Mater. Process.*, 2001, **159**(9), p 49-51
- R.C. Dykhuizen and M.F. Smith, Gas Dynamic Principles of Cold Spray, *J. Therm. Spray Technol.*, 1998, **7**(2), p 205-212
- V.F. Kosarev, S.V. Klinkov, A.P. Alkhimov, and A.N. Papyrin, On Some Aspects of Gas Dynamics of the Cold Spray Process, *J. Therm. Spray Technol.*, 2003, **12**(2), p 265-281
- M. Grujicic, C.L. Zhao, C. Tong, W.S. DeRosset, and D. Helfritsch, Analysis of the Impact Velocity of Powder Particles in the Cold-Gas Dynamic-Spray Process, *Mater. Sci. Eng., A*, 2004, **368**(1), p 222-230
- S.L. Coguill, S.L. Galbraith, D.L. Tuss, M. Ivošević, and L.C. Farrar, U.S. Patent Application 13/506, 215, 2012
- Y. Xu and I.M. Hutchings, Cold Spray Deposition of Thermoplastic Powder, *Surf. Coat. Technol.*, 2006, **201**(6), p 3044-3050
- E. Leivo, T. Wilenius, T. Kinoshita, P. Vuoristo, and T. Mantyla, Properties of Thermally Sprayed Fluoropolymer PVDF, ECTFE, PFA and FEP Coatings, *Prog. Org. Coat.*, 2004, **49**(1), p 69-73
- G. Zhang, W.Y. Li, M. Cherigui, C. Zhang, H. Liao, J.M. Bordes, and C. Coddet, Structures and Tribological Performances of PEEK (Poly-Ether-Ether-Ketone)-Based Coatings Designed for Tribological Application, *Prog. Org. Coat.*, 2007, **60**(1), p 39-44
- C.R. Lima, N.F. de Souza, and F. Camargo, Study of Wear and Corrosion Performance of Thermal Sprayed Engineering Polymers, *Surf. Coat. Technol.*, 2013, **220**, p 140-143
- R. Shahbazi, J. Javadpour, and A.R. Khavandi, Effect of Nanosized Reinforcement Particles on Mechanical Properties of High Density Polyethylene-Hydroxyapatite Composites, *Adv. Appl. Ceram.*, 2006, **105**(5), p 253-257
- P. Bhimaraj, D. Burris, W.G. Sawyer, C.G. Toney, R.W. Siegel, and L.S. Schadler, Tribological Investigation of the Effects of Particle Size, Loading and Crystallinity on Poly (Ethylene) Terephthalate Nanocomposites, *Wear*, 2008, **264**(7), p 632-637
- C. Liu, L. Ren, R.D. Arnell, and J. Tong, Abrasive Wear Behavior of Particle Reinforced Ultrahigh Molecular Weight Polyethylene Composites, *Wear*, 1999, **225**, p 199-204
- E. Kontou and M. Niaounakis, Thermo-mechanical Properties of LLDPE/SiO₂ Nanocomposites, *Polymer*, 2006, **47**(4), p 1267-1280
- J.T. Yeh, H.M. Yang, and S.S. Huang, Combustion of Polyethylene Filled with Metallic Hydroxides and Crosslinkable Polyethylene, *Polym. Degrad. Stab.*, 1995, **50**(2), p p229-p234
- X. Liang, D.M. King, M.D. Groner, J.H. Blackson, J.D. Harris, S.M. George, and A.W. Weimer, Barrier Properties of Polymer/Alumina Nanocomposite Membranes Fabricated by Atomic Layer Deposition, *J. Membr. Sci.*, 2008, **322**(1), p p105-p112
- S.C. Tjong and G.D. Liang, Electrical Properties of Low-Density Polyethylene/ZnO Nanocomposites, *Mater. Chem. Phys.*, 2006, **100**(1), p p1-p5
- K. Ravi, Y. Ichikawa, T. Deplancke, K. Ogawa, O. Lame, and J.Y. Cavaille, Development of Ultra-High Molecular Weight Polyethylene (UHMWPE) Coating by Cold Spray Technique, *J. Therm. Spray Technol.*, 2015, **24**(6), p 1015-1025
- J. Yang, A. Sliva, A. Banerjee, R.N. Dave, and R. Pfeffer, Dry Particle Coating for Improving the Flowability of Cohesive Powders, *Powder Technol.*, 2005, **158**(1), p 21-33



28. W. Lortz, G. Perlet, W. Will, and S. Reitz, U.S. Patent No. 7,834,076, U.S. Patent and Trademark Office, Washington, DC, 2010
29. Z.D. Liu, J.Y. Li, J. Jiang, Z.N. Hong, and R.K. Xu, Adhesion of *Escherichia coli* to Nano-Fe/Al Oxides and its Effect on the Surface Chemical Properties of Fe/Al Oxides, *Colloids Surf., B*, 2013, **110**, p 289-295
30. Technical Information, Degussa AG, Frankfurt, TI 1283
31. Technical Information, Degussa AG, Frankfurt, TI 1340
32. H.D. Chanzy, E. Bonjour, and R.H. Marchessault, Nascent Structures During the Polymerization of Ethylene, *Colloid Polym. Sci.*, 1974, **252**(1), p 8-14
33. S. Rastogi, D.R. Lippits, G.W. Peters, R. Graf, Y. Yao, and H.W. Spiess, Heterogeneity in Polymer Melts from Melting of Polymer Crystals, *Nat. Mater.*, 2005, **4**(8), p 635-641
34. D. Jauffre 's, O. Lame, G. Vigier, and F. Doré, How Nascent Structure of Semicrystalline Polymer Powders Enhances Bulk Mechanical Properties, *Macromolecules*, 2008, **41**(24), p 9793-9801